# Truly Full-Duplex Integrated Sensing and Single-User Communication at mmWave

Murat Bayraktar\*, Nuria González-Prelcic\*, Hao Chen<sup>†</sup>, Charlie Jianzhong Zhang<sup>†</sup>
\*University of California San Diego, USA

†Standards and Mobility Innovation Lab, Samsung Research America, USA

Email: {mbayraktar, ngprelcic}@ucsd.edu, {hao.chen1, jianzhong.z}@samsung.com

Abstract—In this paper, we propose a design for hybrid precoding and combining at mmWave that enables simultaneous monostatic sensing and full-duplex (FD) communication. This joint design mitigates the self-interference (SI) caused by FD operation at the base station (BS). Precoders at the FD BS are designed to maximize signal-to-leakage-plus-noise ratio (SLNR) for downlink (DL) communication and sensing, treating the SI as leakage. The analog combiner minimizes the residual SI at the FD BS under uplink (UL) communication and sensing gain constraints. Moreover, an interference-aware digital combiner separates the target reflections from the UL signals, followed by orthogonal frequency division multiplexing (OFDM) radar for target parameter estimation. Numerical results demonstrate the effectiveness of the proposed design to simultaneously support FD communication and sensing at mmWave.

Index Terms—Full-duplex, self-interference, integrated sensing and communication, hybrid precoding and combining.

#### I. Introduction

Integrated sensing and communication (ISAC) is a key technology to be incorporated in future wireless networks [1]. In particular, mmWave bands can provide high accuracy localization and sensing, enabled by the high resolvability of the channel parameters in the angular and delay domains. Monostatic sensing is one of the possible network sensing modes in ISAC systems [1], requiring a FD circuit to enable reception of the reflections of the transmitted signal on potential targets [2]. The design of FD ISAC systems is challenging, due in part to the impact of the self-interference (SI) introduced by FD operation. Specifically, the SI needs to be suppressed before the analog-to-digital converters (ADCs) of the receiver (RX) end of the FD transceiver.

The design of hybrid precoders and combiners for monostatic ISAC systems at mmWave needs to consider SI mitigation, since this cannot be achieved only by hardware design when the cost is a constraint. Prior work focuses on hybrid precoding/combining for downlink (DL) communication, while the RX end of the FD base station (BS) is employed for monostatic sensing [3]–[6]. These works leverage several SI suppression methods including null-space projection [3], analog SI cancellation [4], iterative convex relaxation [5], [6], and signal-to-leakage-plus-noise ratio (SLNR) precoding [6]. Supporting only DL communication in FD ISAC systems is, however, inefficient, since the FD capability is exploited

This material is based upon work partially supported by the National Science Foundation under grant no. 2147955 and is supported in part by funds from the federal agency and industry partners as specified in the Resilient & Intelligent NextG Systems (RINGS) program and by Samsung Research America.

only for sensing. There are only a few initial works that consider the problem of simultaneous FD communication and sensing [7]–[9]. The designs in [7], [8] exploit a fully digital MIMO architecture, not feasible at mmWave, and only consider the residual SI. The work in [9] considers a hybrid precoder/combiner design with a DL and an uplink (UL) user equipment (UE). However, the channels are assumed to be line-of-sight (LoS), and the UEs are assumed to be the targets, simplifying both the system model and the design problem.

In this paper, we address the simultaneous monostatic sensing and FD communication problem in wideband mmWave MIMO systems with a hybrid analog/digital architecture. We propose a hybrid precoding/combining approach to mitigate SI while providing communication and sensing capabilities. Our contributions include SLNR-based precoding to support DL communication and sensing while suppressing the SI, and an analog combiner design that minimizes the residual SI under UL communication and gain constraints. Numerical results prove that simultaneous UL communication and sensing can be enabled with the proposed design.

## II. SYSTEM MODEL

We consider an ISAC system where the transmitter (TX) end of the FD BS sends data streams to a half-duplex DL UE, while the RX end simultaneously captures the reflections from targets and the data streams transmitted by a half-duplex UL UE. We assume that both the UL and DL communication channels are known, in addition to a coarse estimate of the target angles. There are multiple targets in the environment and we focus on estimating a single target per frame as in [6]–[8]. The system exploits OFDM modulation with M subcarriers and N OFDM symbols per frame. The number of antennas of the collocated TX and RX arrays at the FD BS are denoted by  $N_{\rm BS,T}$  and  $N_{\rm BS,R}$ . The FD BS is equipped with  $N_{\rm BS,RF}$  RF chains at both TX and RX ends. Furthermore, the UEs are equipped with  $N_{\rm UE}$  antennas and  $N_{\rm UE,RF}$  RF chains.

#### A. Channel Models

We leverage a sparse geometric channel model for the DL and UL channels operating at mmWave. Specifically, the channel between the FD BS and the DL UE at the m-th subcarrier is denoted as  $\mathbf{H}_m \in \mathbb{C}^{N_{\mathrm{UE}} \times N_{\mathrm{BS,T}}}$ , and can be written as

$$\mathbf{H}_{m} = \sum_{l=1}^{L_{\mathrm{DL}}} \alpha_{l} e^{-j2\pi m t_{l} \Delta f} \mathbf{a}_{\mathrm{UE}} (\varphi_{l}) \mathbf{a}_{\mathrm{BS,T}}^{\mathrm{H}} (\vartheta_{l}), \qquad (1)$$

where  $L_{\rm DL}$  is the number of paths and  $\Delta f$  is the subcarrier spacing. The complex channel gain, delay, angle-of-arrival (AoA) and angle-of-departure (AoD) of the l-th path are denoted by  $\alpha_l$ ,  $t_l$ ,  $\varphi_l$  and  $\vartheta_l$ , respectively. Furthermore, the array response vectors at UE arrays are represented by  $\mathbf{a}_{\mathrm{UE}}(\phi) \in$  $\mathbb{C}^{N_{\mathrm{UE}}}$  for the incident angle  $\phi$ . Similarly,  $\mathbf{a}_{\mathrm{BS,T}}(\phi) \in \mathbb{C}^{N_{\mathrm{BS,T}}}$ denotes the array response at the TX array of the FD BS. The channel between the UL UE and FD BS at the m-th subcarrier  $\mathbf{G}_m \in \mathbb{C}^{N_{\mathrm{BS,R}} \times N_{\mathrm{UE}}}$  is defined in the same form as (1) with  $L_{\rm UL}$  paths, and complex channel gain, delay, AoA and AoD of the *l*-th path denoted by  $\bar{\alpha}_l$ ,  $\bar{t}_l$ ,  $\bar{\varphi}_l$  and  $\bar{\vartheta}_l$ , respectively. Additionally, the array response vector at the RX array of the FD BS is denoted by  $\mathbf{a}_{BS R}(\phi) \in \mathbb{C}^{N_{BS,R}}$ . We assume that the UL and DL channels remain constant during the coherence time, spanning multiple OFDM frames. For sensing purposes, we exploit a doubly-selective channel model, so that roundtrip delays and Doppler shifts associated to targets can be estimated. Since we consider a monostatic sensing scenario with co-located TX and RX arrays, the AoA and AoD of a target reflection are assumed to be the same [3]–[9]. Thus, the target channel with K targets at the m-th subcarrier of the n-th OFDM symbol  $\mathbf{A}_{m,n} \in \mathbb{C}^{N_{\mathrm{BS},\mathrm{R}} \times N_{\mathrm{BS},\mathrm{T}}}$  is expressed as

$$\mathbf{A}_{m,n} = \sum_{k=0}^{K-1} \beta_k e^{j2\pi(nT_{\mathrm{s}}f_{\mathrm{D},k} - m\tau_k \Delta f)} \mathbf{a}_{\mathrm{BS,R}}(\theta_k) \mathbf{a}_{\mathrm{BS,T}}^{\mathrm{H}}(\theta_k), (2)$$

where  $T_{\rm s}$  is the duration of an OFDM symbol. The complex radar gain, Doppler frequency, round-trip delay, and AoA/AoD of the k-th target are denoted by  $\beta_k$ ,  $f_{D,k}$ ,  $\tau_k$ , and  $\theta_k$ , respectively. The radar gain is characterized by the radar-range equation as  $|\beta_k|^2 = \frac{\lambda^2 \zeta_k}{(4\pi)^3 d_k^4}$ , where  $\lambda$  is the wavelength, while  $\varsigma_k$  and  $d_k$  are the radar cross-section and the range of the k-th target, respectively. Finally, the SI channel is modeled with the near-field LoS model as  $[\mathbf{H}_{\mathrm{SI}}]_{p,q} = \frac{\gamma}{d_{pq}} e^{-j2\pi\frac{d_{pq}}{\lambda}}$ , for  $p=1,\ldots,N_{\mathrm{BS,R}}$  and  $q=1,\ldots,N_{\mathrm{BS,T}}$ , where  $d_{pq}$  is the distance between the p-th RX and q-th TX antenna, and  $\gamma$  is the constant to ensure  $\|\mathbf{H}_{SI}\|_{F}^{2} = N_{BS,T}N_{BS,R}$  [6].

## B. Received Signal Models

In this subsection, we introduce the models for the received signals. The number of data streams transmitted to the DL UE is denoted by  $N_{\rm DL,s}$ . Thus, the data stream transmitted to the DL UE at the m-th subcarrier of the n-th symbol is represented by  $\mathbf{d}_{m,n} \in \mathbb{C}^{N_{\mathrm{DL},s}}$  satisfying  $\mathbb{E}\left\{\mathbf{d}_{m,n}\mathbf{d}_{m,n}^{\mathrm{H}}\right\} = \frac{P_{\mathrm{DL}}}{N_{\mathrm{DL},s}}\mathbf{I}_{N_{\mathrm{DL},s}}$ , where  $P_{\rm DL}$  is the DL transmit power. Additionally, the hybrid precoder at the FD BS for the m-th subcarrier is expressed as  $\mathbf{F}_m = \mathbf{F}_{\mathrm{RF}} \mathbf{F}_{\mathrm{BB},m} \in \mathbb{C}^{N_{\mathrm{BS,T}} \times N_{\mathrm{DL,s}}}$ , with the analog precoder  $\mathbf{F}_{\mathrm{RF}} \in \mathbb{C}^{N_{\mathrm{BS,T}} \times N_{\mathrm{BS,RF}}}$ , and digital precoder  $\mathbf{F}_{\mathrm{BB},m} \in$  $\mathbb{C}^{N_{\mathrm{BS},\mathrm{RF}} \times N_{\mathrm{DL,s}}}$ . The hybrid combiner at the DL UE for the mth subcarrier is defined as  $\mathbf{U}_m = \mathbf{U}_{\mathrm{RF}} \mathbf{U}_{\mathrm{BB},m} \in \mathbb{C}^{N_{\mathrm{UE}} \times N_{\mathrm{DL,s}}}$ , with analog combiner  $\mathbf{U}_{\mathrm{RF}} \in \mathbb{C}^{N_{\mathrm{UE}} \times N_{\mathrm{UE},\mathrm{RF}}}$  and digital combiner  $\mathbf{U}_{\mathrm{BB},m} \in \mathbb{C}^{N_{\mathrm{UE},\mathrm{RF}} \times N_{\mathrm{DL},\mathrm{s}}}$ . With these definitions, the received signal at the DL UE for the m-th subcarrier of the n-th symbol  $\mathbf{r}_{m,n} \in \mathbb{C}^{N_{\mathrm{DL,s}}}$  is written as

$$\mathbf{r}_{m,n} = \mathbf{U}_{m}^{\mathrm{H}} \mathbf{H}_{m} \mathbf{F}_{m} \mathbf{d}_{m,n} + \mathbf{U}_{m}^{\mathrm{H}} \mathbf{z}_{m,n}, \tag{3}$$

 $\mathbf{r}_{m,n} = \mathbf{U}_{m}^{\mathrm{H}} \mathbf{H}_{m} \mathbf{F}_{m} \mathbf{d}_{m,n} + \mathbf{U}_{m}^{\mathrm{H}} \mathbf{z}_{m,n}, \qquad (3)$  where  $\mathbf{z}_{m,n} \in \mathbb{C}^{N_{\mathrm{UE}}}$  is the noise vector with covariance  $\mathbb{E}\left\{\mathbf{z}_{m,n}\mathbf{z}_{m,n}^{\mathrm{H}}\right\} = \sigma_{\mathrm{DL}}^{2} \mathbf{I}_{N_{\mathrm{UE}}}, \text{ being } \sigma_{\mathrm{DL}}^{2} \text{ the noise power.}$ 

We focus on the output of the analog combiner  $\mathbf{W}_{\mathrm{RF}} \in$  $\mathbb{C}^{N_{\mathrm{BS,R}} \times N_{\mathrm{BS,RF}}}$  for the received signal at the FD BS. The data stream transmitted by the UL UE is denoted by  $\mathbf{s}_{m,n} \in \mathbb{C}^{N_{\mathrm{UL,s}}}$ with the covariance  $\mathbb{E}\left\{\mathbf{s}_{m,n}\mathbf{s}_{m,n}^{\mathrm{H}}\right\} = \frac{P_{\mathrm{UL}}}{N_{\mathrm{UL,s}}}\mathbf{I}_{N_{\mathrm{DL,s}}}$ , where  $P_{\mathrm{UL}}$  is the UL transmit power. We define the hybrid precoder at the UL UE for the m-th subcarrier as  $\mathbf{V}_m = \mathbf{V}_{\mathrm{RF}}\mathbf{V}_{\mathrm{BB},m} \in$  $\mathbb{C}^{N_{\mathrm{UE}} \times N_{\mathrm{UL,s}}}$  with  $\mathbf{V}_{\mathrm{RF}} \in \mathbb{C}^{N_{\mathrm{UE}} \times N_{\mathrm{UE,RF}}}$  the frequency-flat analog precoder and  $\mathbf{V}_{\mathrm{BB},m} \in \mathbb{C}^{N_{\mathrm{UE},\mathrm{RF}} imes N_{\mathrm{UL},\mathrm{s}}}$  the digital precoder. Consequently, the received signal at the m-th subcarrier of the *n*-th symbol  $\mathbf{y}_{m,n} \in \mathbb{C}^{N_{\mathrm{UL,s}}}$  can be written as

$$\mathbf{y}_{m,n} = \mathbf{W}_{\mathrm{RF}}^{\mathrm{H}} \mathbf{G}_{m} \mathbf{V}_{m} \mathbf{s}_{m,n} + \mathbf{W}_{\mathrm{RF}}^{\mathrm{H}} \mathbf{A}_{m,n} \mathbf{F}_{m} \mathbf{d}_{m,n} + \sqrt{\rho} \mathbf{W}_{\mathrm{RF}}^{\mathrm{H}} \mathbf{H}_{\mathrm{SI}} \mathbf{F}_{m} \mathbf{d}_{m,n} + \mathbf{W}_{\mathrm{RF}}^{\mathrm{H}} \mathbf{n}_{m,n}, \quad (4)$$

where  $\rho$  is the SI channel power and  $\mathbf{n}_{m,n} \in \mathbb{C}^{N_{\mathrm{BS},\mathrm{R}}}$  is the noise vector with covariance  $\mathbb{E}\left\{\mathbf{n}_{m,n}\mathbf{n}_{m,n}^{\mathrm{H}'}\right\} = \sigma_{\mathrm{BS}}^{2}\mathbf{I}_{N_{\mathrm{BS,R}}}$ , where  $\sigma_{\mathrm{BS}}^{2}$  is the noise power. We define the digital combiner for the UL UE at the m-th subcarrier as  $\mathbf{W}_{\mathrm{BB},m} \in$  $\mathbb{C}^{N_{\mathrm{BS},\mathrm{RF}} \times N_{\mathrm{UL},\mathrm{s}}}$ , and its output  $\bar{\mathbf{y}}_{m,n} \in \mathbb{C}^{N_{\mathrm{UL},\mathrm{s}}}$  as

$$\bar{\mathbf{y}}_{m,n} = \mathbf{W}_{\mathrm{BB},m}^{\mathrm{H}} \mathbf{W}_{\mathrm{RF}}^{\mathrm{H}} \mathbf{G}_{m} \mathbf{V}_{m} \mathbf{s}_{m,n} + \tilde{\mathbf{n}}_{m,n},$$
 (5)

where the interference-plus-noise (IN)  $\tilde{\mathbf{n}}_{m,n} \in \mathbb{C}^{N_{\mathrm{UL,s}}}$  is

$$\tilde{\mathbf{n}}_{m,n} = \mathbf{W}_{\mathrm{BB},m}^{\mathrm{H}} \mathbf{W}_{\mathrm{RF}}^{\mathrm{H}} \left( \mathbf{A}_{m,n} + \sqrt{\rho} \mathbf{H}_{\mathrm{SI}} \right) \mathbf{F}_{m} \mathbf{d}_{m,n} + \mathbf{W}_{\mathrm{BB},m}^{\mathrm{H}} \mathbf{W}_{\mathrm{RF}}^{\mathrm{H}} \mathbf{n}_{m,n}. \quad (6)$$

#### III. PRECODER AND COMBINER DESIGN

In this section, we propose a hybrid precoding and combining framework to support simultaneous monostatic sensing and FD communication for mmWave MIMO systems. We first define the communication and sensing metrics. Then, we define the hybrid precoding and combining problem. Using the DL received signal expression in (3), the spectral efficiency of the DL UE at the m-th subcarrier is expressed as

$$\mathcal{R}_{m} = \log_{2} \left| \mathbf{I}_{N_{\text{DL,s}}} + \frac{P_{\text{DL}}}{N_{\text{DL,s}}} \mathbf{U}_{m}^{\dagger} \mathbf{H}_{m} \mathbf{F}_{m} \mathbf{F}_{m}^{\text{H}} \mathbf{H}_{m}^{\text{H}} \mathbf{U}_{m} \right|, \quad (7)$$

where  $\mathbf{U}_m^\dagger = \left(\mathbf{U}_m^\mathrm{H} \mathbf{U}_m\right)^{-1} \mathbf{U}_m^\mathrm{H}.$  Analogously, using the received signal expression in (5), the spectral efficiency of the UL UE at the m-th subcarrier can be written as

$$\bar{\mathcal{R}}_{m} = \log_{2} \left| \mathbf{I}_{N_{\text{UL,s}}} + \frac{P_{\text{UL}}}{N_{\text{UL,s}}} \mathbf{R}_{\tilde{\mathbf{n}}_{m}}^{-1} \mathbf{W}_{\text{BB},m}^{\text{H}} \mathbf{W}_{\text{RF}}^{\text{H}} \right| \times \mathbf{G}_{m} \mathbf{V}_{m}^{\text{H}} \mathbf{G}_{m}^{\text{H}} \mathbf{W}_{\text{BB},m} \mathbf{W}_{\text{RF}} , \quad (8)$$

where the covariance matrix of the IN vector is defined as  $\mathbf{R}_{\tilde{\mathbf{n}}_m} = \mathbb{E}\left\{\tilde{\mathbf{n}}_{m,n}\tilde{\mathbf{n}}_{m,n}^{\mathrm{H}}\right\} \in \mathbb{C}^{N_{\mathrm{UL,s}} \times N_{\mathrm{UL,s}}}$ . For the sensing metric, we utilize the radar gain at both ends of the FD BS. We track the target with subscript k = 0, thus, the TX and RX radar gains at the target angle  $\theta_0$  are defined as

$$G_{\mathrm{T},m,n_{\mathrm{s}}}(\theta_0) = \left| \mathbf{a}_{\mathrm{BS},\mathrm{T}}^{\mathrm{H}}(\theta_0) \left[ \mathbf{F}_m \right]_{:,n_{\mathrm{s}}} \right|, \tag{9}$$

$$G_{\mathrm{R},n_{\mathrm{RF}}}(\theta_0) = \left| \left[ \mathbf{W}_{\mathrm{RF}} \right]_{:,n_{\mathrm{RF}}}^{\mathrm{H}} \mathbf{a}_{\mathrm{BS},\mathrm{R}}(\theta_0) \right|,$$
 (10)

for  $n_{\rm s}=1,\ldots,N_{\rm DL,s}$ , and  $n_{\rm RF}=1,\ldots,N_{\rm BS,RF}$ , respectively. We also need to define the SI and analog constraints. First, the residual SI at the output of the analog combiner of the FD BS given in (4) should be mitigated, which can be written as  $\mathbf{W}_{\mathrm{RF}}^{\mathrm{H}}\mathbf{H}_{\mathrm{SI}}\mathbf{F}_{m}=\mathbf{0}$ , for  $m=0,\ldots,M-1$ . The analog phase shifter networks require unit modulus entries for the analog precoders/combiners. Except for the combiner at the FD BS, we initially formulate the design of a fully digital solution, enforcing later the hybrid analog/digital structure. We write the overall optimization problem as the maximization of the sum spectral efficiency of the UEs with TX and RX radar gain constraints as

$$\begin{aligned} & \underset{\left\{\mathbf{F}_{m},\mathbf{U}_{m}\right\}_{m},\mathbf{W}_{\mathrm{RF}},}{\text{maximize}} & \sum_{m} \mathcal{R}_{m} + \sum_{m} \bar{\mathcal{R}}_{m} \\ & \left\{\mathbf{V}_{m},\mathbf{W}_{\mathrm{BB},m}\right\}_{m} \\ & \text{subject to} \end{aligned} & G_{\mathrm{T},m,n_{\mathrm{s}}}(\theta_{0}) \geq \tau_{\mathrm{T}}, \ \forall m,n_{\mathrm{s}} \\ & G_{\mathrm{R},n_{\mathrm{RF}}}(\theta_{0}) \geq \tau_{\mathrm{R}}, \ \forall n_{\mathrm{RF}}, \\ & \mathbf{W}_{\mathrm{RF}}^{\mathbf{H}} \mathbf{H}_{\mathrm{SI}} \mathbf{F}_{m} = \mathbf{0}, \ \forall m \\ & \left|\left[\mathbf{W}_{\mathrm{RF}}\right]_{p,q}\right| = 1, \ \forall p,q, \\ & \left\|\left.\mathbf{F}_{m}\right\|_{\mathrm{F}}^{2} = N_{\mathrm{DL,s}}, \ \left\|\mathbf{V}_{m}\right\|_{\mathrm{F}}^{2} = N_{\mathrm{UL,s}}, \ \forall m, \end{aligned}$$

where  $\tau_T$  and  $\tau_R$  are the TX and RX gain thresholds, respectively, whereas the last constraint is the TX power normalization. This problem, even when the hybrid architecture is not enforced, is highly non-linear due to the coupling of the variables. Furthermore, the unit modulus constraint for the analog combiner at the BS makes the problem non-convex. Thus, we sequentially optimize each variable while keeping the others fixed, and we exploit convex relaxation techniques. A. Hybrid Precoder/Combiner Design at the UL/DL UE

The UEs design the optimum precoders/combiners exploiting channel knowledge. The combiner of the DL UE at the m-th subcarrier is initially designed as the first  $N_{\rm DL,s}$  left singular vectors of the DL channel  $\mathbf{H}_m$ . Then, a hybrid factorization technique called phase extraction with alternating minimization is used to find the analog combiner and digital combiners [10]. Analogoulsy, the precoders of the UL UE at the m-th subcarrier are initially obtained from the  $N_{\rm UL,s}$  right singular vectors of the UL channel  $\mathbf{G}_m$ , which is followed by the same hybrid factorization algorithm.

#### B. Hybrid Precoder Design at the FD BS

The design of the precoders at the FD BS can be solved in parallel for all the subcarriers, since we initially assume a fully digital architecture. We further separate the optimization of the communication and sensing metrics. In other words, we design a precoder for communication  $\mathbf{F}_m^{\mathrm{com}} \in \mathbb{C}^{N_{\mathrm{BS,T}} \times N_{\mathrm{DL,s}}}$  and another precoder for sensing  $\mathbf{F}_m^{\mathrm{rad}} \in \mathbb{C}^{N_{\mathrm{BS,T}} \times N_{\mathrm{DL,s}}}$  [3], [6]. Then, we coherently combine these precoders as

$$\mathbf{F}_m = \kappa_1 \mathbf{F}_m^{\text{com}} + (1 - \kappa_1) \mathbf{F}_m^{\text{rad}}, \tag{12}$$

where  $\kappa_1$  controls the trade-off between communication and sensing performance. We normalize the final precoder such that  $\|\mathbf{F}_m\|_{\mathrm{F}}^2 = N_{\mathrm{DL,s}}$ . Furthermore, we utilize a simple search approach to find the largest  $\kappa_1$  value that satisfies the TX gain constraint. The communication precoder design problem for the m-th subcarrier with the SI constraint is expressed as

maximize 
$$\mathcal{R}_m$$
  
subject to  $\mathbf{W}_{\mathrm{RF}}^{\mathrm{H}}\mathbf{H}_{\mathrm{SI}}\mathbf{F}_m^{\mathrm{com}} = \mathbf{0},$  (13)  
 $\left\|\mathbf{F}_m^{\mathrm{com}}\right\|_{\mathrm{F}}^2 = N_{\mathrm{DL,s}}.$ 

Instead of maximizing the spectral efficiency, we propose to maximize the signal-to-leakage-plus-noise (SLNR) ratio,

where the SI is considered to be the leakage. SLNR-based precoding has found many applications in the literature such as multiuser MIMO precoding [11]. The TX signal of the DL UE causes leakage for the received signal at the FD BS in the form of  $\sqrt{\rho}\mathbf{W}_{\mathrm{RF}}^{\mathrm{H}}\mathbf{H}_{\mathrm{SI}}\mathbf{F}_{m}^{\mathrm{com}}\mathbf{d}_{m,n}$  as seen in (4). Then, the SLNR at the m-th subcarrier for the DL UE is expressed as

SLNR<sub>m</sub> = 
$$\frac{\mathbb{E}\left\{\left\|\mathbf{U}_{m}^{H}\mathbf{H}_{m}\mathbf{F}_{m}^{com}\mathbf{d}_{m,n}\right\|^{2}\right\}}{\mathbb{E}\left\{\left\|\sqrt{\rho}\mathbf{W}_{RF}^{H}\mathbf{H}_{SI}\mathbf{F}_{m}^{com}\mathbf{d}_{m,n}\right\|^{2}\right\} + \mathbb{E}\left\{\left\|\mathbf{U}_{m}^{H}\mathbf{z}_{m,n}\right\|^{2}\right\}}$$

$$= \frac{\operatorname{Tr}\left\{\left[\mathbf{F}_{m}^{com}\right]^{H}\mathbf{B}_{m}\mathbf{F}_{m}^{com}\right\}}{\operatorname{Tr}\left\{\left[\mathbf{F}_{m}^{com}\right]^{H}\left(\mathbf{C} + \sigma_{DL}^{2}\mathbf{I}_{N_{BS,T}}\right)\mathbf{F}_{m}^{com}\right\}},$$
(14)

where  $\mathbf{B}_m = \frac{P_{\mathrm{DL}}}{N_{\mathrm{DL,s}}} \mathbf{H}_m^{\mathrm{H}} \mathbf{U}_m \mathbf{U}_m^{\mathrm{H}} \mathbf{H}_m \in \mathbb{C}^{N_{\mathrm{BS,T}} \times N_{\mathrm{BS,T}}}$  and  $\mathbf{C} = \frac{\rho P_{\mathrm{DL}}}{N_{\mathrm{DL,s}}} \mathbf{H}_{\mathrm{SI}}^{\mathrm{H}} \mathbf{W}_{\mathrm{RF}} \mathbf{W}_{\mathrm{RF}}^{\mathrm{H}} \mathbf{H}_{\mathrm{SI}} \in \mathbb{C}^{N_{\mathrm{BS,T}} \times N_{\mathrm{BS,T}}}$ . SLNR maximization for the DL at the m-th subcarrier is given as

$$\begin{array}{ll} \underset{\mathbf{F}_{m}^{\mathrm{com}}}{\operatorname{maximize}} & \mathsf{SLNR}_{m} \\ \mathrm{subject \ to} & \left\|\mathbf{F}_{m}^{\mathrm{com}}\right\|_{\mathrm{F}}^{2} = N_{\mathrm{DL,s}}. \end{array} \tag{15}$$

This is a generalized eigenvalue problem which is equivalently expressed as  $\mathbf{B}_m \mathbf{F}_m^{\mathrm{com}} = \left(\mathbf{C} + \sigma_{\mathrm{DL}}^2 \mathbf{I}_{N_{\mathrm{BS,T}}}\right) \mathbf{F}_m^{\mathrm{com}} \mathbf{\Lambda}_m$ , where the columns of  $\mathbf{F}_m^{\mathrm{com}}$  are the generalized eigenvectors, and  $\mathbf{\Lambda}_m \in \mathbb{C}^{N_{\mathrm{DL,s}} \times N_{\mathrm{DL,s}}}$  is a diagonal matrix that contains the corresponding eigenvalues on its diagonal entries [11]. We design the sensing precoder by using the same methodology. Since the TX radar gain constraint is satisfied with the coherent combination in (12), our goal is to find a precoder that has high TX radar gain while resulting in low residual SI. Hence, we use the same SLNR expression in (14) by only changing the numerator which contains the intended signal power. We take the power of the TX radar gain as the maximization term  $G_{\mathrm{T},m,n_s}^2(\theta_0) = \left[\mathbf{F}_m^{\mathrm{rad}}\right]_{:,n_s}^{\mathrm{H}} \mathbf{a}_{\mathrm{BS,T}}(\theta_0) \mathbf{a}_{\mathrm{BS,T}}^{\mathrm{H}}(\theta_0) \left[\mathbf{F}_m^{\mathrm{rad}}\right]_{:,n_s}^{\mathrm{L}}$ . (16)

The rank of the inner matrix  $\mathbf{a}_{\mathrm{BS,T}}(\theta_0)\mathbf{a}_{\mathrm{BS,T}}^{\mathrm{H}}(\theta_0)$  is 1, thus, we optimize a single vector  $\mathbf{f}_m^{\mathrm{rad}} \in \mathbb{C}^{N_{\mathrm{BS,T}}}$ , and repeat it for the columns of  $\mathbf{F}_m^{\mathrm{rad}}$ . The maximization of sensing SLNR can be formulated by following the same approach in (15), solved as the generalized eigenvalue problem. Finally, we utilize the hybrid factorization algorithm in [10] to find the analog and digital precoders from the fully digital precoders  $\mathbf{F}_m$ .

#### C. Hybrid Combiner Design at the FD BS

The analog combiner at the FD BS should simultaneously provide communication for the UL UE and high RX radar gain. Note that the SI mitigation is the primary goal, since the hybrid factorization applied to the precoders at the FD BS degrades the SI suppression. We propose to define a communication gain constraint similar to the RX radar gain constraint. To that end, we need to find a set of vectors that are useful for communication. This can be achieved by using the eigenvectors that correspond to the  $N_{\rm UL,s}$  largest eigenvalues of the channel covariance matrix  $\frac{1}{M} \sum_m \mathbf{G}_m \mathbf{G}_m^{\rm H}$  to construct  $\mathbf{W}_{\rm RF}^{\rm com} \in \mathbb{C}^{N_{\rm BS,R} \times N_{\rm BS,RF}}$ . If  $N_{\rm BS,RF} > N_{\rm UL,s}$ , the remaining columns can be constructed as a random linear combination of the first  $N_{\rm UL,s}$  columns which are normalized to  $\sqrt{N_{\rm BS,R}}$ . We define the communication gain as  $G_{\rm com,n_{RF}} =$ 

 $|[\mathbf{W}_{\mathrm{RF}}]_{:,n_{\mathrm{RF}}}^{\mathrm{H}}[\mathbf{W}_{\mathrm{RF}}^{\mathrm{com}}]_{:,n_{\mathrm{RF}}}|$ , for  $n_{\mathrm{RF}}=1,\ldots,N_{\mathrm{BS,RF}}$ . We formulate the analog combiner design as the minimization of the total SI with gain constraints. Given the precoders and the unit modulus constraint, this problem can be expressed as

$$\begin{array}{ll} \underset{\mathbf{W}_{\mathrm{RF}}}{\text{minimize}} & \sum_{m} \left\| \mathbf{W}_{\mathrm{RF}}^{\mathrm{H}} \mathbf{H}_{\mathrm{SI}} \mathbf{F}_{m} \right\|_{\mathrm{F}}^{2} \\ \text{subject to} & G_{\mathrm{R}, n_{\mathrm{RF}}}(\theta_{0}) \geq \tau_{\mathrm{R}}, \ \forall n_{\mathrm{RF}}, \\ & G_{\mathrm{com}, n_{\mathrm{RF}}} \geq \tau_{\mathrm{com}}, \ \forall n_{\mathrm{RF}}, \\ & \left| \left[ \mathbf{W}_{\mathrm{RF}} \right]_{p,q} \right| = 1, \ \forall p, q, \end{array}$$

where  $\tau_{\rm com}$  is the communication gain threshold. This problem is non-convex due to the unit modulus constraint. Additionally, the gain constraints are non-convex, which can be circumvented by writing them as gain loss constraints, defined as

$$|N_{\rm BS,R} - [\mathbf{W}_{\rm RF}]_{:,n_{\rm RF}}^{\rm H} \mathbf{a}_{\rm BS,R}(\theta_0)| \le (N_{\rm BS,R} - \tau_{\rm R}), \quad (18)$$

$$|N_{\rm BS,R} - [\mathbf{W}_{\rm RF}]_{:,n_{\rm RF}}^{\rm H} [\mathbf{W}_{\rm RF}^{\rm com}]_{:,n_{\rm RF}}| \le (N_{\rm BS,R} - \tau_{\rm com}). \quad (19)$$

To overcome the non-convexity of the unit modulus constraint, we limit the deviation of the entries of the combiner  $\mathbf{W}_{RF}$  from the unit circle as done in [5], [6]. We utilize a random block coordinate descent method such that a certain number of randomly selected entries are optimized at each iteration until the convergence is achieved. The overall evolution of the combiner is limited to prevent missing the local minima. The convex problem solved at the t-th iteration is expressed as

minimize 
$$\begin{bmatrix} \mathbf{W}_{\mathrm{RF}} \mathbf{I}_{\mathcal{I}_{t}} & \sum_{m} \left\| \mathbf{W}_{\mathrm{RF}}^{\mathrm{H}} \mathbf{H}_{\mathrm{SI}} \mathbf{F}_{m} \right\|_{\mathrm{F}}^{2}$$
subject to (18), (19),  $\forall n_{\mathrm{RF}}$ ,
$$\left| \begin{bmatrix} \mathbf{W}_{\mathrm{RF}} \end{bmatrix}_{p,q} \right| - 1 \leq \epsilon_{1}, \ (p,q) \in \mathcal{I}_{t},$$

$$\left\| \begin{bmatrix} \mathbf{W}_{\mathrm{RF}} \end{bmatrix}_{\mathcal{I}_{t}} - \begin{bmatrix} \mathbf{W}_{\mathrm{RF}}^{(t-1)} \end{bmatrix}_{\mathcal{I}_{t}} \right\| \leq \epsilon_{2},$$
(20)

where  $\epsilon_1$  and  $\epsilon_2$  are small threshold values. Moreover, the set of randomly selected indices at the t-th iteration is denoted by  $\mathcal{I}_t$ . The entries optimized at the t-th iteration are represented by  $[\mathbf{W}_{\mathrm{RF}}]_{\mathcal{I}_t} \in \mathbb{C}^{|\mathcal{I}_t|}$ , whereas the analog combiner optimized at the (t-1)-th iteration is denoted by  $\mathbf{W}_{\mathrm{RF}}^{(t-1)}$ . At the end of each iteration, the entries are normalized to unity. The problem (20) is solved with the convex solver CVX [12]. The initialization of this solution is the coherent combination of the communication and sensing combiners given as

$$\mathbf{W}_{\mathrm{RF}}^{\mathrm{init}} = \kappa_2 \mathbf{W}_{\mathrm{RF}}^{\mathrm{com}} + (1 - \kappa_2) \mathbf{W}_{\mathrm{RF}}^{\mathrm{rad}}, \tag{21}$$

where the sensing combiner  $\mathbf{W}_{\mathrm{RF}}^{\mathrm{rad}} \in \mathbb{C}^{N_{\mathrm{BS,R}} \times N_{\mathrm{BS,RF}}}$  is constructed as  $\mathbf{W}_{\mathrm{RF}}^{\mathrm{rad}} = \left[\mathbf{a}_{\mathrm{BS,R}}(\theta_0), \ldots, \mathbf{a}_{\mathrm{BS,R}}(\theta_0)\right]$ . Moreover,  $\kappa_2$  is the trade-off parameter for communication and sensing, and the entries of the initial combiner are normalized to unity. We assume that the SI is jointly suppressed by the precoders and the analog combiner utilized at the FD BS. Additionally, we assume that the interference caused by the target reflections is weak. Thus, we set the digital combiner  $\mathbf{W}_{\mathrm{BB},m}$  as the left singular vectors that correspond to the  $N_{\mathrm{UL,s}}$  largest singular values of the equivalent UL channel  $\mathbf{W}_{\mathrm{RF}}\mathbf{G}_m\mathbf{V}_m$ .

## IV. PARAMETER ESTIMATION FOR MONOSTATIC SENSING

In this section, we introduce the techniques for target parameter estimation. We first leverage an interference-aware filter to separate the target reflections from the UL signal. Then, we utilize OFDM radar for range-velocity estimation. Since we are only interested in a single target, we rewrite the received signal in (4) by separating the target reflection as

$$\mathbf{y}_{m,n} = \bar{\beta}_{0,m,n} \mathbf{W}_{\mathrm{RF}}^{\mathrm{H}} \mathbf{a}_{\mathrm{BS,R}}(\theta_0) \mathbf{a}_{\mathrm{BS,T}}^{\mathrm{H}}(\theta_0) \mathbf{F}_m \mathbf{d}_{m,n} + \mathbf{n}_{m,n}^{0},$$
(22)

where  $\bar{\beta}_{0,m,n}=\beta_0 e^{j2\pi(nT_{\rm s}f_{{\rm D},0}-m\tau_0\Delta f)}$ , and  ${\bf n}_{m,n}^0\in\mathbb{C}^{N_{{\rm BS,RF}}}$  contains the IN terms. The interference from the other targets are assumed to be much weaker than the reflections of the intended target. We define the radar combiner for the m-th subcarrier as  ${\bf w}_m\in\mathbb{C}^{N_{{\rm BS,RF}}}$  which is designed by using the minimum variance distortionless response (MVDR) beamformer approach [13]. The MVDR solution is given as

$$\mathbf{w}_{m} = \frac{\mathbf{R}_{\bar{\mathbf{n}}_{m}}^{-1} \mathbf{W}_{RF}^{H} \mathbf{a}_{BS,R}(\theta_{0})}{\mathbf{a}_{BS,R}^{H}(\theta_{0}) \mathbf{W}_{RF} \mathbf{R}_{\bar{\mathbf{n}}_{m}}^{-1} \mathbf{W}_{RF}^{H} \mathbf{a}_{BS,R}(\theta_{0})}, \quad (23)$$

where  $\bar{\mathbf{n}}_{m,n}^0 \in \mathbb{C}^{N_{\mathrm{BS,RF}}}$  is the interference vector without the target interference, and  $\mathbf{R}_{\bar{\mathbf{n}}_m^0} \in \mathbb{C}^{N_{\mathrm{BS,RF}} \times N_{\mathrm{BS,RF}}}$  is its covariance matrix. Let us express the signal at the output of the MVDR beamformers as

$$y_{m,n}^{\text{rad}} = \bar{\beta}_{0,m,n} \mathbf{w}_m^{\text{H}} \mathbf{W}_{\text{RF}}^{\text{H}} \mathbf{a}_{\text{BS,R}}(\theta_0) \mathbf{a}_{\text{BS,T}}^{\text{H}}(\theta_0) \mathbf{F}_m \mathbf{d}_{m,n} + \mathbf{w}_m^{\text{H}} \mathbf{n}_{m,n}^0.$$
(24)

The radar signal-to-interference-plus-noise ratio (SINR) at the m-th subcarrier of the n-th OFDM symbol is expressed as

$$\mathsf{SINR}_{m,n} = \frac{\beta_0^2 P_{\mathrm{DL}} \left\| \mathbf{w}_m^{\mathrm{H}} \mathbf{W}_{\mathrm{RF}}^{\mathrm{H}} \mathbf{a}_{\mathrm{BS,R}}(\theta_0) \mathbf{a}_{\mathrm{BS,T}}^{\mathrm{H}}(\theta_0) \mathbf{F}_m \right\|^2}{N_{\mathrm{DL,s}} \left| \mathbf{w}_m^{\mathrm{H}} \mathbf{R}_{\mathbf{n}_{m,n}^0} \mathbf{w}_m \right|^2}, (25)$$

where  $\mathbf{R}_{\mathbf{n}_{m,n}^0}$  is the covariance matrix of the IN term in (22). In the context of ISAC, OFDM has been studied extensively, mainly due to its wide adoption in commercial communication systems [3], [4], [6]. In this paper, we also exploit OFDM radar technique for joint range-velocity estimation. We firstly cancel the effect of the scalar which is in product form with  $\bar{\beta}_{0,m,n}$  in (24), and construct the image  $\mathbf{Z} \in \mathbb{C}^{M \times N}$  as

$$[\mathbf{Z}]_{m,n} = \frac{y_{m,n}^{\text{rad}}}{\mathbf{w}_{m}^{\text{H}} \mathbf{W}_{\text{RF}}^{\text{H}} \mathbf{a}_{\text{BS,R}}(\theta) \sum_{i=1}^{U_{\text{DL}}} \mathbf{a}_{\text{BS,T}}^{\text{H}}(\theta) \mathbf{F}_{m} \mathbf{d}_{m,n}}. (26)$$

We take the DFT over the rows and inverse DFT over the columns of  $\mathbf{Z}$ . The indices of the peak location can be converted to range and velocity estimates as in [4], [6]. It is shown that the residual UL signal diminishes with large M and N since the DL and UL symbols are independent [7].

# V. Numerical Results

In this section, we evaluate the ISAC performance of the proposed design. The BS is equipped with two uniform linear arrays separated by  $6\lambda$  with  $N_{\rm BS,T}=N_{\rm BS,R}=64$  antennas, whereas the UEs are equipped with  $N_{\rm UE}=16$  antennas. The spacing between the antenna elements is half wavelength. The number of RF chains and the number of streams at the BS and UEs are 4. The system operates at 28GHz with a 100MHz bandwidth corresponding to a noise power of  $-93.8 {\rm dBm}$  at room temperature. The number of subcarriers and OFDM symbols are set to M=792 and N=14, with subcarrier spacing  $\Delta f=120{\rm kHz}$  and symbol duration  $T_{\rm s}=8.92 \mu {\rm s}$  [4]. We consider K=4 point targets with radar cross-section of  $10{\rm m}^2$ .

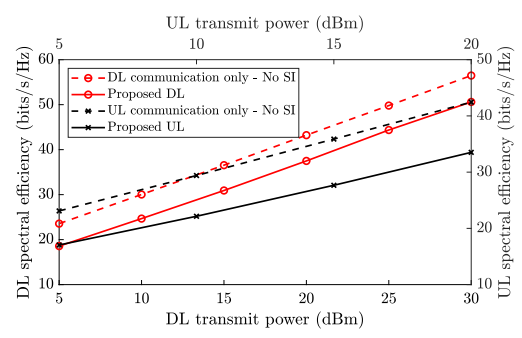


Fig. 1. Spectral efficiency of DL/UL UE with respect to transmit power at SI-to-noise ratio  $\rho/\sigma_{\rm BS}^2=80{\rm dB}$ .

The target angles are randomly selected from  $[-60^\circ, 60^\circ]$ . The range of the target of interest is set to 40m while the range of other targets are randomly selected from [20m, 60m]. Velocity of the targets are randomly selected from [10m/s, 30m/s]. The UEs are deployed 50m away from the BS with the LoS angle selected from  $[-60^\circ, 60^\circ]$ . The channels consist of 5 paths. The gains of NLoS paths are 5-15dB below the gain of the LoS path, while the angles are randomly selected from  $[-90^\circ, 90^\circ]$ . The TX/RX gain and communication gain thresholds are set to  $\tau_T = \tau_R = 0.4 N_{\rm BS,R}$  and  $\tau_{\rm com} = 0.5 N_{\rm BS,R}$ , respectively. The design parameters are set to  $\epsilon_1 = 0.3$ ,  $\epsilon_2 = 0.1$  and  $\epsilon_2 = 0.5$ . In addition, 30% of the entries are optimized at every iteration of the analog combiner design.

Fig. 1 shows the DL and UL spectral efficiencies as a function of the transmit power. The UL spectral efficiency is calculated considering the interference generated by a DL transmit power set to 20dBm. We use the half-duplex communication without sensing as baseline. It can be seen that the proposed design provides high DL and UL spectral efficiency while enabling simultaneous sensing capabilities and suppressing the SI as shown next. The spectral efficiency can be increased if the radar gain thresholds are decreased.

To evaluate the sensing performance, Fig. 2 shows the radar SINR as a function of the SI-to-noise ratio and the empirical CDFs of the velocity and range estimates. We compare the radar SINR of the proposed design with the case without the UL UE, the case with matched filter (MF) instead of MVDR, and the case where there is no SI suppression. The latter case uses the eigenvector-based precoders and the initial analog combiner. It can be observed that the proposed design is robust to SI-to-noise ratio as high as 100dB, and the usage of the MVDR beamformer significantly enhances the performance. Furthermore, the CDF of the velocity and range estimation errors with QPSK symbols show that accurate parameter estimation can be achieved in the presence of the UL signals. However, we observe that the number of OFDM symbols affects the performance, especially with UL signals.

## VI. CONCLUSION

In this paper, we proposed an SI-aware hybrid precoding/combining architecture for joint radar sensing and FD communication in mmWave systems. We exploited SLNR-based precoding and an iterative convex relaxation-based analog combiner solution to jointly suppress the SI while simulta-

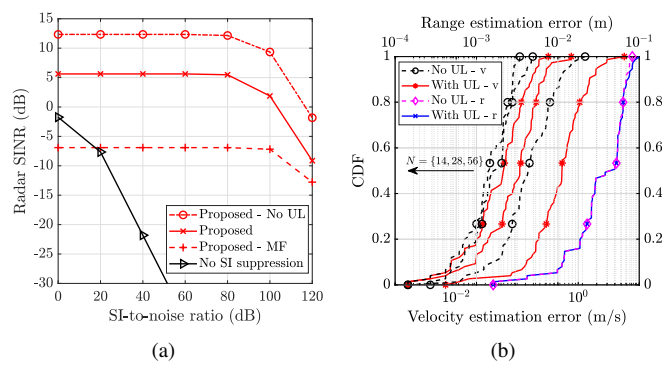


Fig. 2. Sensing results with  $P_{\rm DL}=20{\rm dBm}$  and  $P_{\rm UL}=10{\rm dBm}$ : (a) Radar SINR vs SI-to-noise ratio, (b) CDF of range and velocity estimation errors at SI-to-noise ratio  $\rho/\sigma_{\rm BS}^2=80{\rm dB}$ .

neously satisfying sensing and communication requirements. We leveraged the beamspace MVDR beamformer to separate the target reflections from the UL signals, while the range and velocity of the targets are estimated with OFDM radar. The simulation results show the robustness of the proposed solution to strong SI, and the potential to estimate the target parameters in the presence of UL signals.

#### REFERENCES

- N. González-Prelcic, M. F. Keskin, O. Kaltiokallio, M. Valkama, D. Dardari, X. Shen, Y. Shen, M. Bayraktar, and H. Wymeersch, "The integrated sensing and communication revolution for 6G: Vision, techniques, and applications," *Proceedings of the IEEE*, 2024.
- [2] C. B. Barneto, S. D. Liyanaarachchi, M. Heino, T. Riihonen, and M. Valkama, "Full duplex radio/radar technology: The enabler for advanced joint communication and sensing," *IEEE Wireless Commun.*, vol. 28, no. 1, pp. 82–88, 2021.
- [3] C. B. Barneto, T. Riihonen, S. D. Liyanaarachchi, M. Heino, N. González-Prelcic, and M. Valkama, "Beamformer design and optimization for joint communication and full-duplex sensing at mm-Waves," *IEEE Trans. Commun.*, vol. 70, no. 12, pp. 8298–8312, 2022.
- [4] M. A. Islam, G. C. Alexandropoulos, and B. Smida, "Integrated sensing and communication with millimeter wave full duplex hybrid beamforming," in *Proc. IEEE Int. Conf. Commun. (ICC)*, 2022, pp. 4673–4678.
- [5] M. Bayraktar, C. Rusu, N. González-Prelcic, and H. Chen, "Self-interference aware codebook design for full-duplex joint sensing and communication systems at mmWave," in *Proc. IEEE 9th Int. Workshop Comput. Adv. Multi-Sensor Adaptive Process.*, 2023, pp. 231–235.
- [6] M. Bayraktar, N. González-Prelcic, and H. Chen, "Hybrid precoding and combining for mmWave full-duplex joint radar and communication systems under self-interference," in *Proc. IEEE Int. Conf. Commun.* (ICC), 2024, pp. 1–6.
- [7] Z. Liu, S. Aditya, H. Li, and B. Clerckx, "Joint transmit and receive beamforming design in full-duplex integrated sensing and communications," *IEEE J. Sel. Areas Commun.*, vol. 41, no. 9, pp. 2907–2919, 2023.
- [8] Z. He, W. Xu, H. Shen, D. W. K. Ng, Y. C. Eldar, and X. You, "Full-duplex communication for ISAC: Joint beamforming and power optimization," *IEEE J. Sel. Areas Commun.*, vol. 41, no. 9, pp. 2920– 2936, 2023.
- [9] M. Talha, B. Smida, M. A. Islam, and G. C. Alexandropoulos, "Multi-target two-way integrated sensing and communications with full duplex MIMO radios," arXiv preprint arXiv:2312.10345, 2023.
- [10] X. Yu, J.-C. Shen, J. Zhang, and K. B. Letaief, "Alternating minimization algorithms for hybrid precoding in millimeter wave MIMO systems," *IEEE J. Sel. Top. Signal Process.*, vol. 10, pp. 485–500, 2016.
- [11] M. Sadek, A. Tarighat, and A. H. Sayed, "A leakage-based precoding scheme for downlink multi-user MIMO channels," *IEEE Trans. Wireless Commun.*, vol. 6, no. 5, pp. 1711–1721, 2007.
- [12] M. Grant and S. Boyd, "CVX: Matlab software for disciplined convex programming, version 2.1," 2014.
- [13] H. L. Van Trees, Optimum array processing: Part IV of detection, estimation, and modulation theory. John Wiley & Sons, 2002.